Histograms of Helicity and Strain in Numerical Turbulence

Robert M. Kerr
Geophysical Turbulence Program, National Center for Atmospheric Research, Boulder, Colorado 80307
(Received 30 January 1987)

Histograms of the normalized values of the helicity and the smallest principal component of the rate of strain are found for one realization of a 128^3 isotropic simulation of forced turbulence. In regions of high dissipation the strain has a structure indicating sheets. Peak-to-valley ratios in the helicity histograms are less than in other numerical flows and this ratio decreases further when the helical large scales are filtered or active regions characterized by the strain are sampled.

PACS numbers: 47.25.-c, 47.30.+s

To investigate the alignment of vorticity and strain and to study recent claims[1,2] concerning the importance of helicity in numerical turbulence this Letter analyzes historgrams of helicity and strain for a simulation of forced turbulence.[3] Helicity could impose a constraint on solutions of the Euler equations because it is a second quadratic invariant of the Euler equations in addition to the kinetic energy and because it is related to the nonlinear term in the rotational form of the Navier-Stokes equation

$$\frac{\partial \mathbf{u}}{\partial t} = \mathbf{u}\times\boldsymbol{\omega} - \nabla\left(\frac{P}{\rho} + \frac{1}{2}\mathbf{u}^2\right) + \nu\nabla^2\mathbf{u} \tag{1}$$

by $|u^2||\omega^2| = |\mathbf{u}\cdot\boldsymbol{\omega}|^2 + |\mathbf{u}\times\boldsymbol{\omega}|^2$, where $\boldsymbol{\omega} = \nabla\times\mathbf{u}$ is the vorticity. It has been suggested that the invariance of helicity increases the probability of the flow being Beltrami type; that is that the normalized helicity

$$\cos(\theta) = \mathbf{u}\cdot\boldsymbol{\omega}/|\mathbf{u}||\boldsymbol{\omega}| \tag{2}$$

is ± 1, because in regions where this is true the relative nonlinear term is small and the kinetic-energy cascade is inhibited. It has also been suggested that because the normalized helicity is not Galilean invariant these concepts are not applicable for general nonhomogeneous turbulent flows.[4] To examine these predictions experimentally both the velocity and vorticity would have to be measured simultaneously, a difficult but not impossible task that has been attempted.[5] It is much easier to do the analysis with a numerical simulation, where all of the flow information is known, but in that case there can be questions about whether the calculation is at high enough Reynolds number to allow one to comment on the influence of helicity on small-scale turbulence.

Some numerical flows where the probability density of the normalized helicity has been presented are a channel flow,[1] a particular time in a Taylor-Green flow,[1] and decaying turbulence in a periodic box.[2] Strong peaks for the normalized helicity of the nonfluctuating velocity and vorticity at ± 1 are observed in the center of the 32^3 channel[1] but not throughout the channel. The Taylor-Green flow shows strong peaks in the helicity histogram at ± 1 in regions of low dissipation, but again not throughout the flow. Helicity profiles for decaying turbulence on a 32^3 mesh[2] are strongly peaked at ± 1, independent of initial conditions. A more recent analysis of numerical sheared and strained turbulence with up to 128^3 nodes[6] and of channel flow with $192\times129\times160$ nodes does not show any indication of large normalized helicity.[7]

It has also been suggested[8] that the helicity within bands in Fourier space has a strong peak at ± 1. If these bands are within the inertial subrange, it would suggest a local Beltrami character that might inhibit the nonlinear terms responsible for the turbulent energy cascade. While the helicity structure within Fourier bands is not thoroughly investigated in this Letter, the helicity distribution for structures associated with the turbulent cascade is reported.

In addition to historgrams of normalized helicity, this Letter will consider histograms of the smallest eigenvalue of the rate of strain and of vortex stretching. To analyze the strain, histograms of

$$A = \sqrt{6}\beta/|e_{ij}| \tag{3}$$

are plotted, where $\alpha+\beta+\gamma=0$, with $\alpha>\beta>\gamma$, are the eigenvalues of the strain tensor $e_{ij} = \frac{1}{2}\{\partial u_i/\partial x_j + \partial u_j/\partial x_i\}$ and $|e_{ij}| = (\sum_{i,j} e_{ij}^2)^{1/2}$ is the absolute magnitude of this tensor. Related quantities that have been analyzed[9] are histograms of vortex stretching,

$$B = (\tfrac{3}{2})^{1/2}\omega_i e_{ij}\omega_j/|\omega^2||e_{ij}|, \tag{4}$$

$$C = \sqrt{6}e_{ij}e_{jk}e_{ki}/|e_{ij}|^{3/2}, \tag{5}$$

and the angle between the eigenvector $\boldsymbol{\beta}$ associated with the smallest component of the rate of strain β and the vorticity,

$$D = \boldsymbol{\beta}\cdot\boldsymbol{\omega}/|\boldsymbol{\omega}|. \tag{6}$$

All of these quantities have been normalized such that they lie between -1 and 1. $\omega_i e_{ij}\omega_j$ is the rate of production of ω^2 and, on the assumption of isotropy,[10] is related to the velocity-derivative skewness

$$S_u = \langle(\partial u_1/\partial x_1)^3\rangle\langle(\partial u_1/\partial x_1)^2\rangle^{-3/2} \tag{7}$$

by

$$\tfrac{35}{2}(\partial u_1/\partial x_1)^3 = -\omega_i e_{ij}\omega_j. \quad (8)$$

C is related to the smallest component of the rate of strain by

$$C = -\tfrac{1}{2}A(3-A^2), \quad (9)$$

and on the assumption of homogeneity and isotropy,[10] C is related to S_u by

$$\tfrac{35}{2}(\partial u_1/\partial x_1)^3 = \tfrac{4}{3}e_{ij}e_{jk}e_{ki}. \quad (10)$$

All of the results to be presented are from one time realization of a 128^3 forced pseudospectral simulation of the incompressible Navier-Stokes equation in a three-dimensional periodic box.[3] The analysis has been repeated with other realizations and identical results are obtained to within statistical error. The simulation was intended to represent statistically steady isotropic turbulence. To maintain the kinetic energy the velocity was forced by keeping the kinetic energy in the first band of wave numbers constant, with the modes in the first band interacting with each other through the nonlinear terms. Analysis of the dependence of the higher-order derivative statistics in this calculation[3] showed agreement with experiments, suggesting that this simulation is a good representation of the small scales of turbulence for the Taylor-microscale Reynolds number R_λ up to 83. One decade of the Kolmogorov $k^{-5/3}$ was observed. The statistics and graphics suggested that the strongest eigenvectors of the rate-of-strain tensor would be compressive and aligned perpendicular to the vorticity. The structure of the strain field will be presented first so as to define the conditional sampling used for the helicity.

Since the α component of the rate of strain is always greater than 0 and γ is always less than 0, historgrams of the β component of the rate of strain are considered because the sign of β determines whether the local structure of turbulence is sheetlike or tubelike. If β is greater than 0 then there are two components of the rate of strain along which the fluid is stretching and one component along which it is being compressed, which suggests that the local structure will be sheetlike. If β is less than 0 then there will be two compressive components and one stretching component of the rate of strain, which suggests tubelike structures. A third possibility is that $\beta=0$, which indicates that the flow is locally two dimensional.

Figure 1 plots the historgram of the normalized β strain A. For all the historgrams to be presented there are eighty bins between -1 and 1. The histograms of A have been normalized such that their integral is 1. The peak in Fig. 1 is at $\frac{1}{2}$, which is equivalent to values of (α,β,γ) that go as $(3,1,-4)$. This is consistent with the observation[3] that the compressive component of the rate of strain tends to be largest. By (9) this implies that a histogram of C should peak at negative values, which by (10) would be necessary to ensure a negative value of S_u. This is found, with the peak of the histogram of C at -1.

Conditional samples based on the dissipation being 2 and 4 times its mean are also shown in Fig. 1. These samples represent 10% and 3% of the nodes. The tendency for A to be greater than 0 becomes more pronounced where the dissipation is large and suggests that the dissipative structures of turbulence are sheets. Vortex sheets are a product of an inviscid Taylor-Green calculation,[11] and a recent calculation[12] with the code used here shows that two oppositely directed vortex filaments evolve into a dissipative structure characterized by a double vortex sheet.

Because of vortex stretching, the vorticity should be aligned with positive components of the rate of strain, that is with $\boldsymbol{\alpha}$ or $\boldsymbol{\beta}$, the eigenvectors associated with the α and β components of the strain. The histogram of D is strongly peaked at ± 1; that is, $\boldsymbol{\beta}$ is aligned with the vorticity $\boldsymbol{\omega}$, with 25% of the points having $|D|>0.925$ over the entire flow and more than 60% of the points with $|D|>0.925$ when the flow is conditionally sampled for the dissipation 4 times its mean. If it is assumed that the vorticity and $\boldsymbol{\beta}$ are perfectly aligned, then the histogram of A between -1 and 1 maps onto the histogram of B between -0.5 and 0.5. Figure 1 shows the histogram of B between -0.5 and 0.5 (shown as the histogram of $2B$ between -1 and 1) to demonstrate this. Histograms of B when the flow is conditionally sampled based upon the value of A have confirmed the relationship between A and B. Because B is formed from the nonlinear terms in the vorticity equation associated with vortex stretching and the turbulent cascade, the relation between A and B suggests that the structures responsible for the turbulent cascade are sheetlike.

It has been shown[9] for the forced flow[3] and a numerical homogeneous shear flow[5] that as the value of the dissipation used for conditionally sampling A is raised, there is an asymptotic profile for the histogram that peaks at $A=0.5$. To demonstrate a possible connection between these histograms and the derivative statistics calculated before,[3] assume that A is 0.5 everywhere and B is 0.25 everywhere. If vorticity and strain are assumed to be uniformly distributed, then by (3) and (10) S_u is -0.48, in good agreement with the value actually calculated. This shows that at least one derivative statistic can be predicted solely upon arguments for alignment of the small scales, without reference to intermittency.

Figure 2 plots histograms of the helicity without conditional sampling, without conditional sampling but with the first two wave-number shells[3] filtered out, conditional sampling based on the dissipation greater than 4 times its mean, and conditional sampling based on whether A is less than 0 or greater than 0.75, that is whether the flow is tubelike with low dissipation or strongly sheetlike and dissipative. The histograms have been normalized such that $P(1)=1$. The conditional samples over A are

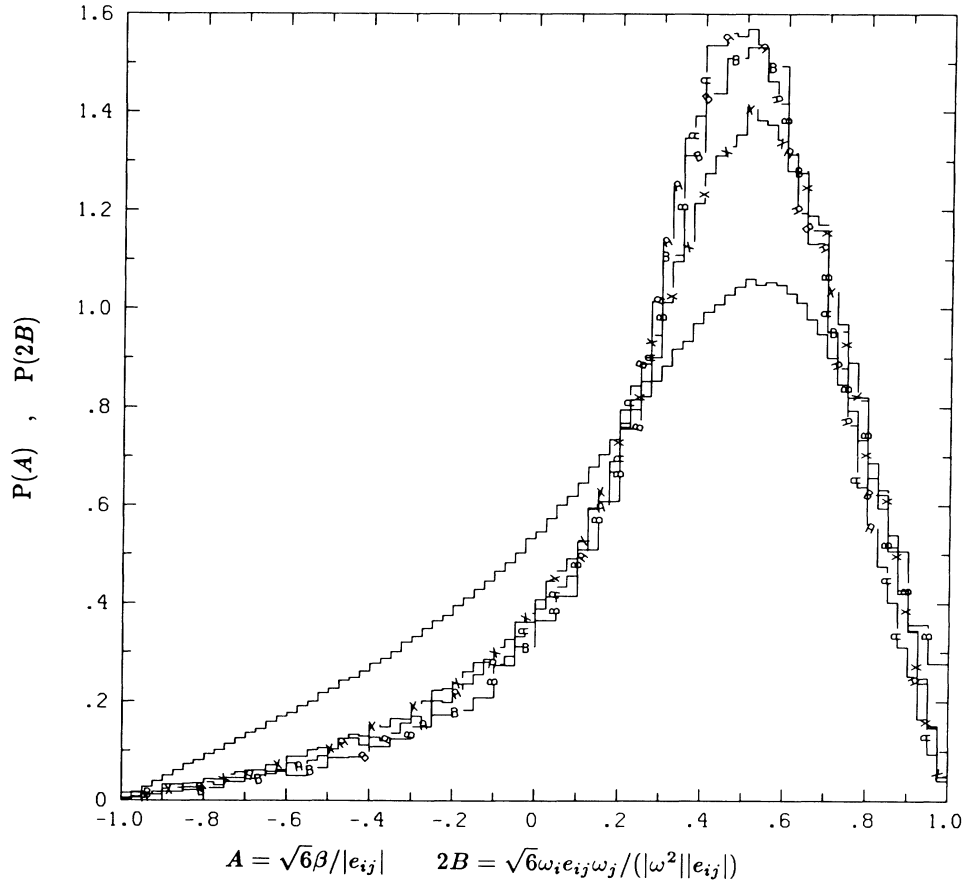

FIG. 1. Histograms of the normalized β strain A, unlabeled histogram, over the entire flow; X, A conditioned by the dissipation greater than twice its mean; A, A conditioned by the dissipation greater than 4 times its mean; and histogram, B, of twice the normalized vortex stretching $2B$ conditioned by the dissipation greater than 4 times its mean. The area under each curve is 1.

over 20% and 10% of the nodes, respectively. The asymmetry that appears in the histogram for the entire field is due to the helicity in the forcing modes, which is maintained throughout the calculation. Some of the helicity from the forcing is transferred to the second wave number, but very little is found in higher wave numbers. For comparison the helicity in the first four shells is 5.22, 2.59, 0.33, and -0.21 and the product of the magnitude of the velocity $|u| = (2E)^{1/2}$ and the vorticity $|\omega|$ in those shells is $|u||\omega| = 7.70$, 5.82, 5.00, and 3.57, which is consistent with the $-\frac{5}{3}$ subrange plotted previously.[3] Figure 2 shows that most of the asymmetry disappears when the first two wave-number shells are filtered from the analysis. This filter does not significantly affect the historgrams in Fig. 1. Since the higher modes contribute the most to vortex stretching and turbulent production, this suggests that Beltrami flows are not important in small-scale turbulent production. When a suggested anisotropic wave-number filter[8] is applied the asymmetry in the normalized helicity distribution is greater, but is not significantly different from that generated by random distributions.[8] Coincidentally, the only experimental attempt to measure the helicity distribution[5] has the same asymmetry and peak-to-valley ratio as the overall distribution of this calculation.

Although the peak-to-valley ratio of the overall normalized helicity histogram for this flow is much smaller than earlier analyses,[1,2] it is significant enough that its source should be studied further. Figure 2 shows that $\cos(\theta) = +1$ is more likely in regions where the local energy dissipation $\epsilon = |e_{ij}|^2 + \frac{1}{2}\boldsymbol{\omega}^2$ is large. Conditional sampling based upon the kinetic energy, strain squared, or enstrophy produces similar histograms. It should be noted that none of these second-order quantities is a direct measure of where the turbulent cascade is taking place or where the nonlinear terms are large. Figure 1 suggests that a better indication of the active parts of turbulent is the sign of A. Conditional sampling based on the value of A shows a clear trend toward less symmetry and a smaller peak-to-valley ratio in sheetlike regions. Conditional sampling based on where the cosine of the angle between $\boldsymbol{\beta}$ and $\boldsymbol{\omega}$, D, is near ± 1 does not show any clear trends.

The conclusion of this analysis is that while there is

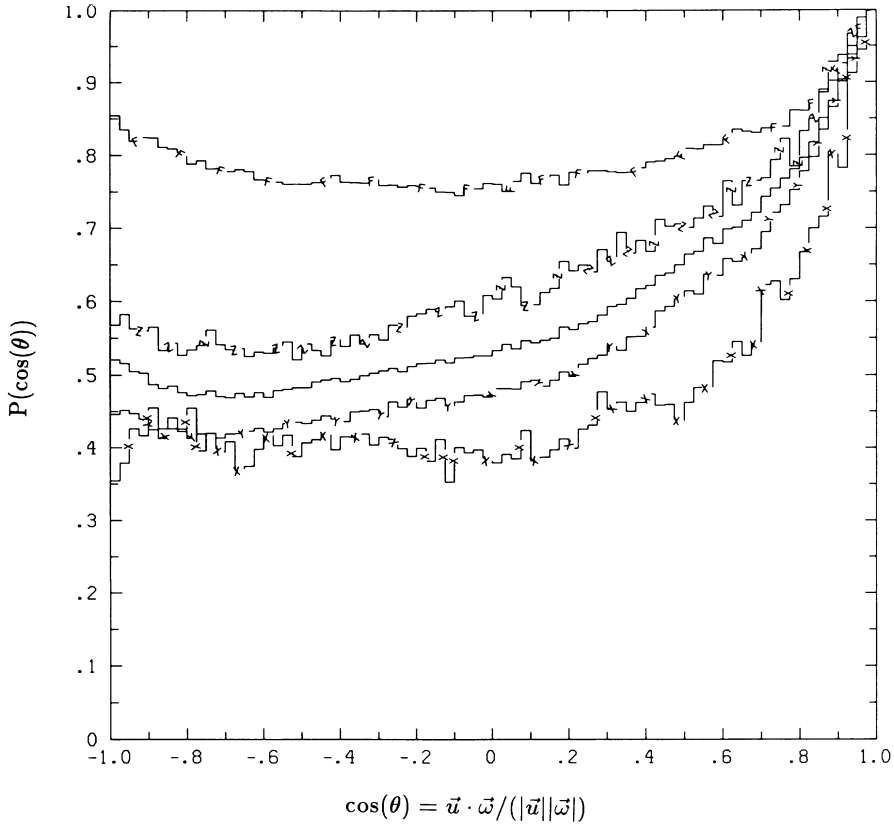

FIG. 2. Histograms of the normalized helicity $\cos(\theta)$, unlabeled histogram, over the entire flow: F, with first two wave-number shells filtered; X, conditioned by the dissipation greater than 4 times its mean; Y, conditioned by A less than 0.0; and Z, conditioned by A greater than 0.75. Each curve is normalized such that $P(1)=1$.

not good evidence for strong alignment between the velocity and vorticity or a large normalized helicity, there is strong evidence for a difference type of alignment. This alignment between the vorticity and strain and the evidence for a universal distribution for the strain in regions of high dissipation suggests a characteristic sheetlike structure for the dissipative regions or turbulence. Where this sheetlike structure is strongest, there is evidence that the influence of helicity is even smaller. Evidence was presented that this sheetlike structure is related to the nonlinear terms responsible for vortex stretching and the cascade of energy to small scales. While Fig. 2 shows regions of the flow with enhanced normalized helicity, there is no evidence that these regions are directly involved in the turbulent cascade.

I wish to thank W. Ashurst for his suggestions. This work has been supported by the U.S. Army Research Office at the National Center for Atmospheric Research. The National Center for Atmospheric Research is sponsored by the National Science Foundation. Computational support from the NASA Ames Research Center is acknowledged.

[1]R. B. Pelz, V. Yakhot, S. A. Orszag, L. Shtilman, and E. Levich, Phys. Rev. Lett. **54**, 2505 (1985).

[2]R. B. Pelz, L. Shtilman, and A. Tsinober, Phys. Fluids. **29**, 3506–3508 (1986).

[3]R. M. Kerr, J. Fluid Mech. **153**, 31–58 (1985).

[4]C. G. Speziale, Quart. Appl. Math. **45**, 123–129 (1987).

[5]J. L. Balint, P. S. Bernard, L. Vukoslavevic, and J. M. Wallace, Bull. Am. Phys. Soc. **31**, 1685 (1986).

[6]M. M. Rogers, P. Moin, and W. C. Reynolds, Stanford University Report No. TF-25, 1986 (unpublished).

[7]M. M. Rogers and P. Moin, "Helicity in Incompressible Turbulent Flows" (to be published).

[8]V. Yakhot, S. Orszag, A. Yakhot, R. Panda, U. Frisch, and R. Kraichnan, "Weak Interactions and Local Order in Strong Turbulence" (to be published).

[9]W. T. Ashurst, A. R. Kerstein, R. M. Kerr, and C. H. Gibson, "Alignment of Vorticity and Scalar Gradient with Strain Rate in Simulated Navier-Stokes Turbulence" (to be published).

[10]E. D. Siggia, Phys. Fluids **107**, 357–406 (1981).

[11]M. E. Brachet, D. I. Meiron, S. A. Orszag, B. G. Nickel, R. H. Morf, and U. Frisch, J. Fluid Mech. **130**, 411–452 (1983).

[12]A. Pumir and R. M. Kerr, Phys. Rev. Lett. **58**, 1636–1639 (1987).